Available online at www.sciencedirect.com
ScienceDirect
Trans. Nonferrous Met. Soc. China 34(2024) 3749−3761
Transactions of Nonferrous Metals Society of China
www.tnmsc.cn

Preparation of low-oxygen titanium powder by magnesiothermic reduction of TiO_2 assisted by $MgCl_2$−$HoCl_3$ molten salt

Li-guo ZHU[1,2,3,4#], Chong-lin BAI[1,2,3,4#], Ling-xin KONG[1,2,3,4], Bin YANG[1,2,3,4], Bao-qiang XU[1,2,3,4]

1. Key Laboratory for Nonferrous Vacuum Metallurgy of Yunnan Province, Kunming University of Science and Technology, Kunming 650093, China;
2. State Key Laboratory of Complex Non-ferrous Metal Resources Clean Utilization, Kunming University of Science and Technology, Kunming 650093, China;
3. National Engineering Research Center of Vacuum Metallurgy, Kunming University of Science and Technology, Kunming 650093, China;
4. Faculty of Metallurgical and Energy Engineering, Kunming University of Science and Technology, Kunming 650093, China

Received 16 June 2023; accepted 21 March 2024

Abstract: To reduce the production cost of titanium, a new method for direct preparation of low-oxygen titanium powder by the magnesiothermic reduction of TiO_2 with the assistance of a $MgCl_2$−$HoCl_3$ molten salt was proposed. Thermodynamic calculations showed that the magnesiothermic reduction of TiO_2 was feasible. However, hindrance of the reduction reaction by the reduction by-product of MgO resulted in a considerably high O concentration in the titanium powder. The addition of $HoCl_3$ to the system significantly reduces the activity of MgO to produce low-oxygen titanium powder. Thermochemical deoxidation and reduction experiments were conducted with $MgCl_2$−$HoCl_3$ molten salt in the temperature range of 1023−1273 K. The results showed that titanium powder with oxygen concentration (mass fraction) below 5.00×10^{-4} can be prepared at the Mg−$MgCl_2$−HoOCl−$HoCl_3$ equilibrium.
Key words: titanium powder; $MgCl_2$−$HoCl_3$ molten salt; TiO_2; HoOCl; magnesiothermic reduction

1 Introduction

Ti is an abundant resource. Ti and its alloys contain only Al and Fe in common structural metals because of their favorable properties such as low mass, high specific strength, corrosion resistance, heat resistance, and biocompatibility [1−4]. The Kroll process, in which $TiCl_4$ is used as the raw material and Mg as the reducing agent, can be employed to produce high-purity products and is easily industrialized [5,6]. The Kroll process is the main method used for the large-scale industrial production of Ti sponges, which have become the most important raw materials for Ti powder and ingots. However, despite nearly 50 years of process optimization and application development, the Kroll process still suffers from drawbacks such as high energy and monetary costs, and heavy pollution. These deficiencies significantly restrict the development of the Ti industry [7,8].

Following the initial proposal of the Kroll process in the 1940s, several alternative economical processes were developed. Thermochemical reduction

# Li-guo ZHU and Chong-lin BAI contributed equally to this work
Corresponding author: Ling-xin KONG, Tel: +86-15987180307, E-mail: kkmust@126.com; Bin YANG, Tel: +86-871-65161583, E-mail: kgyb2005@126.com
DOI: 10.1016/S1003-6326(24)66638-0
1003-6326/© 2024 The Nonferrous Metals Society of China. Published by Elsevier Ltd & Science Press
This is an open access article under the CC BY-NC-ND license (http://creativecommons.org/licenses/by-nc-nd/4.0/)

is a promising process [9−14]. In thermochemical reduction, $TiCl_4$ and TiO_2 are used as the main raw materials for Ti. The advantage of using $TiCl_4$ as a raw material is that the residual impurities such as Mg, $MgCl_2$, and $TiCl_2$ can be removed via vacuum distillation to produce high-purity Ti. However, the production of pure $TiCl_4$ is energy-consuming and expensive [15]. The use of TiO_2 produced using sulfate or chloride as a raw material is another economical and effective method for producing Ti. Because of the strong affinity of Ti for O, TiO_2 can only be reduced by metals with strong reducibility such as Ca, Mg, Al, and Li [16]. Ca and Mg are ideal reducing agents that are available from a wide range of sources with low cost.

SUZUKI and INOUE [17] studied the preparation of Ti powder via the calciothermic reduction of TiO_2. According to the Ca−$CaCl_2$−CaO phase diagram, a Ti powder with an O concentration of less than 1.00×10^{-3} (mass fraction, the same below) was obtained at 1173 K; however, the Ca concentration in the product was higher than that of Ti (>1.00×10^{-3}). OKABE et al [18] proposed a preformed reduction process (PRP) that was used to produce 99% pure Ti powder. Although the amount of $CaCl_2$ in the product was acceptable, the concentrations of O $(2.00-3.00)\times10^{-3}$) and Ca (1.00×10^{-3}) were extremely high. XU et al [19−21] studied the reduction of TiO_2 using Ca vapor to obtain a Ti powder with an O concentration of 1.00×10^{-3}. Although Ca as a reducing agent can be used to produce Ti powder with a low O concentration, separating the metal from the molten salt was difficult.

Magnesium has a significant advantage owing to its low cost and ability to reduce TiO_2 at lower temperatures compared to other reducing agents [22]. NERSISYAN et al [23] obtained a Ti powder with an O concentration of 1.50×10^{-2} through the magnesiothermic reduction of TiO_2 by combustion synthesis. The product was further deoxidized using Ca to reduce the O concentration in the Ti powder to $(2.00-3.00)\times10^{-3}$. However, this process is time-consuming and inefficient. FAN et al [24] prepared Ti powder through the multistage reduction of Mg using a self-propagating method. Although this process was used to produce Ti powder with an O concentration of 2.35×10^{-3}, significant deoxidation by Ca was required. The low chemical affinity between Mg and O hampered Mg deoxidation. The high O concentration in the Ti powder obtained by directly reducing TiO_2 by Mg required further deoxidation by Ca, resulting in a long processing time and low efficiency.

Low-O Ti powder can also be prepared via the calciothermic reduction of TiO_2 owing to the high solubility of CaO in $CaCl_2$ (the solubility of CaO is 20 mol.% at 1173 K) [25]. However, the significantly lower solubility of MgO in $MgCl_2$ (the solubility of MgO is 1.5 mol.% at 1173 K) [25] results in the attachment of MgO to the Ti oxide surface. This hinders Mg reduction and results in excessive O concentration in the product. Therefore, during TiO_2 reduction, the MgO deoxidation by-products must be dissolved by physical or chemical methods to remove excessive oxygen and obtain a low-O Ti powder. To achieve this, a method was proposed, in which the activity of MgO (a_{MgO}) was effectively reduced and maintained at a low level adding $RECl_3$ (RE=Y, Ho) to the molten salt to promote deoxidation of the Ti powder.

Although rare earth metals are considered scarce resources, there are abundant reserves of approximately 4×10^5 t Ho [26]. By continuously optimizing the Ho production process, the amount of Ho produced could surpass that used in the future [27]. Therefore, Ho has high application potential [28].

This study aims to prepare low-O Ti powder through the magnesiothermic reduction of TiO_2 with $HoCl_3$ molten salt to provide a new method for preparing of low-O Ti powders and opens up a novel direction for utilizing Ho. Additionally, the new method has a short processing time and low cost, which effectively reduces the cost of Ti powder.

2 Thermodynamic analysis

Table 1 lists the standard Gibbs energy changes for the compound formation and O dissolved in β-Ti at various temperatures [28−30].

Figure 1 shows Ellingham diagram of various metal oxides drawn based on Ref. [29].

As shown in Fig. 1, MgO is more stable than Ti oxide. In addition, Mg and Ti did not form alloys or compounds. Therefore, it is feasible to prepare Ti powder via the magnesiothermic reduction of TiO_2.

Table 1 Standard Gibbs energy changes ($\Delta G^{\Theta}_{f,i}$) of formation of compounds and O dissolved in β-Ti

Compound	$\Delta G^{\Theta}_{f,i}$	Temperature range/K
$HoCl_3$(l)	$\Delta G^{\Theta}_{f,i}$ =−952950+193.26T	1000−1300
HoOCl(s)	$\Delta G^{\Theta}_{f,i}$ =−991900+172.8T	1100−1500
MgO(s)	$\Delta G^{\Theta}_{f,i}$ =−608270+115.49T	900−1300
$MgCl_2$(l)	$\Delta G^{\Theta}_{f,i}$ =−594108+111.69T	1000−1300
Ho_2O_3(s)	$\Delta G^{\Theta}_{f,i}$ =−1864755+273.05T	900−1500
TiO_2(s)	$\Delta G^{\Theta}_{f,i}$ =−940913+177.83T	298−2000
Ti_4O_7(s)	$\Delta G^{\Theta}_{f,i}$ =−3382590+600.16T	298−2000
Ti_3O_5(s)	$\Delta G^{\Theta}_{f,i}$ =−2434056+420.46T	298−2000
Ti_2O_3(s)	$\Delta G^{\Theta}_{f,i}$ =−1504815+260.65T	298−2000
TiO(s)	$\Delta G^{\Theta}_{f,i}$ =−538529+90.94T	298−2000
$MgTiO_3$(s)	$\Delta G^{\Theta}_{f,i}$ =−1572943+293.45T	900−1300
$MgTi_2O_5$(s)	$\Delta G^{\Theta}_{f,i}$ =−2505838+462.21T	900−1300
Mg_2TiO_4(s)	$\Delta G^{\Theta}_{f,i}$ =−2172020+396.24T	900−1300
[O] in Ti[a]	$\Delta G^{\Theta}_{f,i}$ =−583000+88.5T	1173−1373

[a]1/2 O_2 (g) = [O] in Ti (1 wt.%), i.e. Henrian's 1 wt.% standard

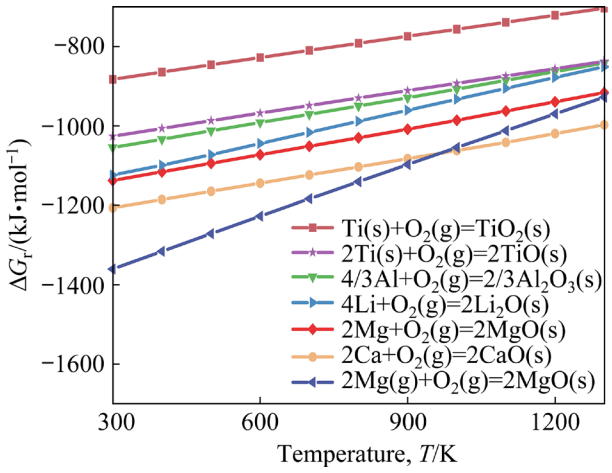

Fig. 1 Ellingham diagram of some metal oxides (ΔG_r is Gibbs free energy change of reactions) [29]

This reaction can be described as follows:

$$2Mg(l)+TiO_2(s)=Ti(s)+2MgO(s) \quad (1)$$

The Mg−Ti−O ternary phase diagram at 1023 K, drawn using the data in Table 1, is shown in Fig. 2.

The coexistence of Mg, Ti, and MgO phases suggests that Ti can be prepared by reducing TiO_2 with Mg. The reduction of TiO_2 is a complex process in which the side reactions MgO+TiO_2→$MgTi_2O_5$ ($MgTiO_3$, Mg_2TiO_4) may occur. The attachment of the MgO by-product, and the $MgTiO_3$ and Mg_2TiO_4 intermediate products to the surface of the reactants significantly hinders the reduction reaction. Although Ti powder can be prepared through the magnesiothermic reduction of TiO_2, the obtained Ti powder contains a considerable concentration of O. By reducing the activity of MgO, the efficiency of the magnesiothermic reduction of TiO_2 can be significantly improved to produce low-O Ti powder efficiently.

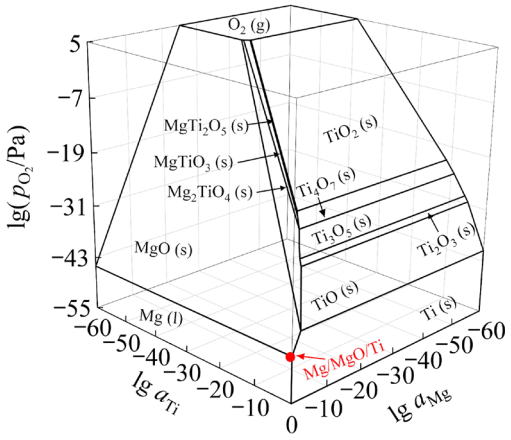

Fig. 2 Ternary phase diagram of Mg−Ti−O system at 1023 K (a_{Mg} is activity of magnesium, a_{Ti} is activity of titanium, and p_{O_2} is oxygen partial pressure)

The relationship between the activity of MgO (a_{MgO}) and the O concentration in β-Ti can be obtained using Eqs. (2) and (3):

$$Mg(l)+1/2O_2(g)=MgO(s) \quad (2)$$

$$\Delta G^{\Theta}_r = -2.303RT\lg\left(\frac{a_{MgO}}{a_{Mg}\cdot p^{1/2}_{O_2}}\right) \quad (3)$$

where R is the molar gas constant (8.314 J/(mol·K)), and T is the thermodynamic temperature, K.

Equation (4) can be derived from Eq. (3):

$$\lg p_{O_2} = 2\lg a_{MgO} + \frac{2\Delta G^{\Theta}_r}{2.303RT} - 2\lg a_{Mg} \quad (4)$$

The relationship between the concentration of O dissolved in β-Ti and p_{O_2} can be expressed by Eqs. (5)−(7):

$$1/2O_2(g)=O(\text{in } \beta\text{-Ti, 1 wt.\%}) \quad (5)$$

$$\Delta G^{\Theta}_{l,Ti} = -2.303RT\lg[(f_O\cdot[O]_{Ti})/p^{1/2}_{O_2}] \quad (6)$$

$$\Delta G^{\Theta}_{l,Ti} = -583000+88.5T \ (T=1173-1373\ K) \quad (7)$$

where $\Delta G^{\Theta}_{l,Ti}$ is the Gibbs energy change of the standard reaction of O dissolved in Ti (1 wt.% solution as the standard state); $[O]_{Ti}$ is the O concentration in Ti; f_O is the Henry activity coefficient. O dissolved in β-Ti obeys Henry's law, and f_O=1.

Equations (8) and (9) are obtained by combining Eqs. (2), (3), (5) and (6):

$$Mg(l)+O(\text{in }\beta\text{-Ti, 1 wt.\%})=MgO(s) \quad (8)$$

$$\lg(f_O\cdot[O]_{Ti})+\frac{\Delta G^{\Theta}_{l,Ti}}{2.303RT}=\lg a_{MgO}+\frac{\Delta G^{\Theta}_{r}}{2.303RT}-\lg a_{Mg} \quad (9)$$

from which it can be derived that

$$\lg(f_O\cdot[O]_{Ti})=\lg a_{MgO}+\frac{\Delta G^{\Theta}_{r}}{2.303RT}-\frac{\Delta G^{\Theta}_{l,Ti}}{2.303RT}-\lg a_{Mg} \quad (10)$$

The relationship between the temperature and O concentration in β-Ti was calculated for the a_{MgO} values of 0.001, 0.01, 0.1, and 1 using Eq. (10) and the data listed in Table 1 and Fig. 3. Some data were obtained by extrapolation and showed errors within the allowed range.

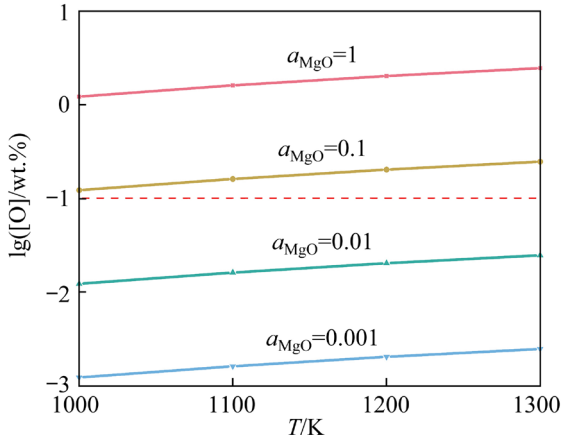

Fig. 3 Relationship between temperature and O concentration in β-Ti at Mg−MgO equilibrium and excess Mg (a_{Mg}=1)

Figure 3 shows that at Mg−MgO equilibrium and excess Mg (a_{Mg}=1), decreasing the temperature for a given MgO activity decreases the O concentration in β-Ti. For instance, when the MgO activity (a_{MgO}) is 1, the O concentrations in β-Ti at 1023, 1073, 1123, 1173, 1223, and 1273 K are 1.32×10^{-2}, 1.51×10^{-2}, 1.72×10^{-2}, 1.92×10^{-2}, 2.14×10^{-2}, and 2.36×10^{-2}, respectively. Moreover, decreasing the activity of MgO (a_{MgO}) decreases the oxygen concentration in β-Ti. For example, the O concentration in β-Ti is lower than 1.00×10^{-3} when a_{MgO} falls below 0.1.

Figure 3 also shows that at Mg−MgO equilibrium and excess Mg (a_{Mg}=1), the O concentration in β-Ti is affected by both the temperature and MgO activity, with the latter being the main factor. This suggests that low-O Ti powder can be prepared directly by reducing the activity of MgO (a_{MgO}) using physical or chemical methods. However, reducing the a_{MgO} using $MgCl_2$ effectively is challenging because of the low solubility of MgO in $MgCl_2$ (1.5 mol.% at 1173 K). This reduces the effectiveness of the reduction and deoxidation processes, making it difficult to obtain low-O Ti. To address this problem, the rare-earth metal Ho or its chloride ($HoCl_3$) can be added to the $MgCl_2$ system to reduce the activity of the deoxidation by-product MgO ($MgO(s)+HoCl_3(l)=HoOCl(s)\downarrow+MgCl_2(l)$) to obtain low-O Ti powder.

Using the thermodynamic data listed in Table 1, a $\lg p_{Cl_2}$−$\lg p_{O_2}$ diagram at 1023 K for M−Cl−O (M=Ho, Mg) system is calculated and plotted in Fig. 4. Here, p_{Cl_2} is the partial pressure of Cl_2.

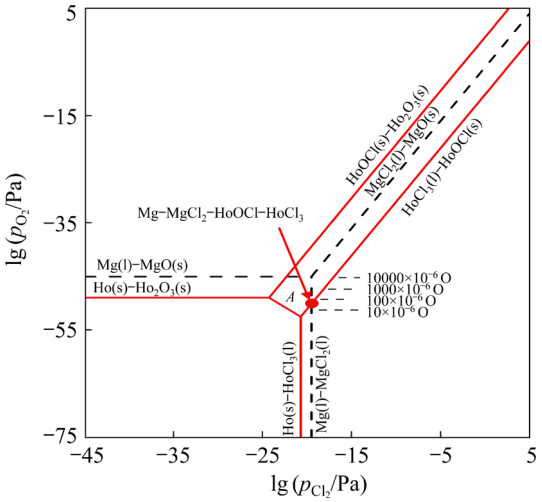

Fig. 4 $\lg p_{O_2}$−$\lg p_{Cl_2}$ diagram of M−Cl−O (M=Ho, Mg) system at 1023 K

As shown in Fig. 4, p_{O_2} at intersection Point *A* (Mg−$MgCl_2$−$HoCl_3$−HoOCl equilibrium), which is the intersection of the Mg−$MgCl_2$ and $HoCl_3$−HoOCl equilibria, can be obtained as follows:

$1/2O_2(g)+Mg(l)+HoCl_3(l)=MgCl_2(l)+HoOCl(s)$ (11)

$$\Delta G^{\Theta}_{r,(11)} = -2.303RT\lg\left(\frac{a_{MgCl_2}\cdot a_{HoOCl}}{a_{Mg}\cdot a_{HoCl_3}\cdot p_{O_2}^{1/2}}\right) \quad (12)$$

$$\Delta G^{\Theta}_{r,(11)} = \Delta G^{\Theta}_{f,HoOCl} + \Delta G^{\Theta}_{f,MgCl_2} - \Delta G^{\Theta}_{f,HoCl_3} \quad (13)$$

The p_{O_2} at the Mg−$MgCl_2$−HoOCl−$HoCl_3$ equilibrium (1023 K, 7.8×10^{-51} Pa) is considerably lower than that at the Mg−MgO equilibrium (1023 K, 9.0×10^{-46} Pa).

By combining Eqs. (5) and (11), the deoxidation limit of the Mg−$MgCl_2$−HoOCl−$HoCl_3$ equilibrium system was calculated as follows:

O(in β-Ti)+$Mg(l)+HoCl_3(l)=MgCl_2(l)+HoOCl(s)$ (14)

$$\Delta G^{\Theta}_{deox,\ Mg-MgCl_2-HoOCl-HoCl_3} = -2.303RT\lg\frac{a_{MgCl_2}\cdot a_{HoOCl}}{a_{Mg}\cdot a_{HoCl_3}\cdot f_O\cdot[O]_{Ti}} \quad (15)$$

$$\Delta G^{\Theta}_{deox,\ Mg-MgCl_2-HoOCl-HoCl_3} = \Delta G^{\Theta}_{f,HoOCl} + \Delta G^{\Theta}_{f,MgCl_2} - \Delta G^{\Theta}_{f,HoCl_3} - \Delta G^{\Theta}_{l,Ti} \quad (16)$$

The deoxidation limits (a_{MgCl_2}=1, a_{Mg}=1, a_{HoCl_3}=1, a_{HoOCl}=1) of Mg−$MgCl_2$−HoOCl−$HoCl_3$ were calculated using Eqs. (15) and (16). At 1023 K and Mg−$MgCl_2$−HoOCl−$HoCl_3$ equilibrium, the O concentration in β-Ti is 3.80×10^{-5}, which is considerably lower than that in β-Ti (1.32×10^{-2}) at Mg−MgO equilibrium.

When the activities of Mg (l) and HoOCl (s), and f_O are 1, Eq. (15) becomes

$$\lg[O]_{Ti} = \lg\frac{a_{MgCl_2}}{a_{HoCl_3}} + \frac{\Delta G^{\Theta}_{deox,Mg-MgCl_2-HoOCl-HoCl_3}}{2.303RT} \quad (17)$$

The relationship between the O concentration and the activity of $HoCl_3$ at 1023, 1073, 1123, 1173, 1223, and 1273 K at the Mg−$MgCl_2$−HoOCl−$HoCl_3$ equilibrium was calculated and plotted using Eq. (17), as shown in Fig. 5.

As shown in Fig. 5, when the activities of $HoCl_3$ are 0.003, 0.003, 0.004, 0.004, 0.005, and 0.005, the deoxidation limits are 1.32×10^{-2}, 1.51×10^{-2}, 1.72×10^{-2}, 1.93×10^{-2}, 2.14×10^{-2}, and 2.36×10^{-2} at 1023, 1073, 1123, 1173, 1223, and 1273 K, respectively, and the Mg−$MgCl_2$−HoOCl−$HoCl_3$ equilibrium is achieved in the system. After reaching Mg−$MgCl_2$−HoOCl−$HoCl_3$ equilibrium, the deoxidation limit decreases as the activity of $HoCl_3$ increases. Additionally, at 1023, 1073, 1123,

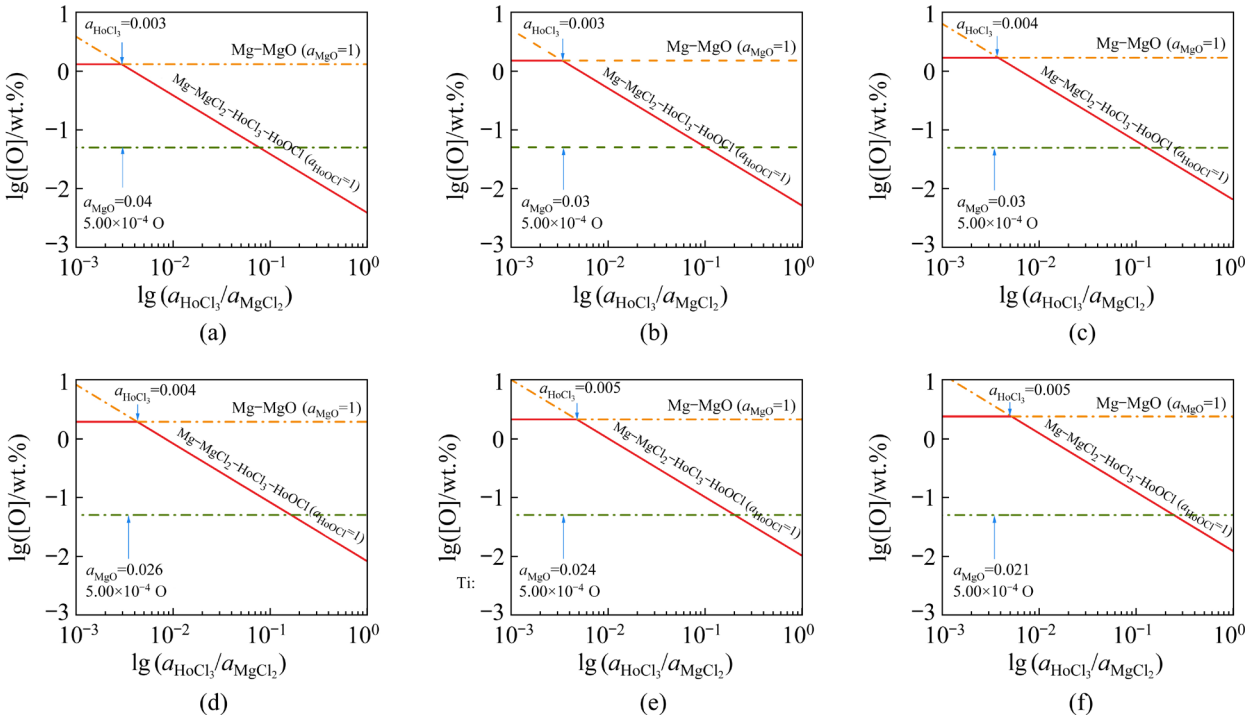

Fig. 5 Relationship between O concentration in Ti and a_{HoCl_3}/a_{MgCl_2} at a_{Mg}=1, Mg−$MgCl_2$−HoOCl−$HoCl_3$ equilibrium and different temperatures: (a) 1023 K; (b) 1073 K; (c) 1123 K; (d) 1173 K; (e) 1223 K; (f) 1273 K

1173, 1223, and 1273 K, the activities of MgO are 0.04, 0.03, 0.03, 0.026, 0.024, and 0.021, respectively, and the deoxidation limit is 5.00×10^{-4}. This indicates that the thermodynamic deoxidation limit at low temperatures is lower than that at high temperatures and that low temperatures are more conducive to deoxidation. Therefore, the magnesiothermic reduction of TiO_2 can be used to prepare Ti powder with an O concentration below 5.00×10^{-4} using a $HoCl_3$ molten salt at the $Mg-MgCl_2-HoOCl-HoCl_3$ equilibrium.

3 Experimental

3.1 Materials

Table 2 lists the chemical reagents and materials used in the experiments.

As shown in Fig. 5, when the activities of $HoCl_3$ are 0.003, 0.003, 0.004, 0.004, 0.005, and 0.005, the $Mg-MgCl_2-HoOCl-HoCl_3$ equilibrium is achieved at 1023, 1073, 1123, 1173, 1223, and 1273 K, respectively. Table 3 lists the initial amounts of the raw materials in the Ti crucible used in the thermochemical experiment.

The effect of the $HoCl_3$ activity on the O concentration in the Ti samples was investigated in Experiments $1^{\#}$–$5^{\#}$, and the effect of the $HoCl_3$ activity on the O concentration in Ti powder was investigated in Experiment $6^{\#}$. Ti samples were used in Experiments $1^{\#}$–$5^{\#}$, whereas Ti and TiO_2 were used in Experiment $6^{\#}$.

3.2 Process and equipment

Figure 6 [31] shows the experimental setup used in this study. Before the experiment, TiO_2 and 30 wt.% NH_4HCO_3 were fully mixed with an appropriate amount of ethylcellulose. The mixture was pressed into round sheets (0.4 g) with a diameter of 13 mm and a thickness of approximately 2 mm under a pressure of 15 MPa. A high-temperature resistance furnace (Shanghai Yifeng Resistance Furnace Co., Ltd., China) was used to sinter the samples at 1273 K for 4 h to obtain loose and porous TiO_2 sheets.

Table 2 Chemical reagents and experimental materials

Chemical reagent or experimental material	Form	Purity/grade	Supplier
TiO_2	Powder	99.5%	Nangong Jiannuo Trade Co., Ltd.
$MgCl_2$	Powder	99.5%	Shanghai McLean Biochemical Technology Co., Ltd.
Ho	Shot	99.9%	Zhongnuo Advanced Material (Beijing) Technology Co., Ltd.
Mg	Shot	99.95%	Tianjin Metal Material Sales Co., Ltd.
NH_4HCO_3	Powder	99.7%	Shanghai Aladdin Biochemical Technology Co., Ltd.
Ethylcellulose	Powder	99.7%	Shanghai Aladdin Biochemical Technology Co., Ltd.
Ti-A	Wire with 2 mm in diameter	~9.60×10^{-4} O	Shanxi Weixiangrui Metal Materials Co., Ltd.
Ti-B	Wire with 3 mm in diameter	~1.30×10^{-3} O	Shanxi Weixiangrui Metal Materials Co., Ltd.
Ti	Sponge	97%	Guantai Metal Materials Co., Ltd.
Ti crucible	25.4 mm in diameter; 80 mm in height; 1 mm in thickness	CP-Ti[a]	Shanxi Weixiangrui Metal Materials Co., Ltd.
Stainless-steel crucible	88.8 mm in diameter; 106 mm in height; 3 mm in thickness		Dongguan Hongyuanda Metal Products Co., Ltd.
Ti foil	0.1 mm in thickness	CP-Ti[a]	Shanxi Weixiangrui Metal Materials Co., Ltd.

[a] Commercially pure Ti (~ 99.5%)

Table 3 Initial amounts of raw materials in Ti crucible

Exp. No.	Initial amount/g(mol)		Theoretical content of $HoCl_3$ in molten salt/mol.%
	$MgCl_2$	Ho	
1	9.52(0.1)	1.57(0.010)	10
2	9.52(0.1)	4.30(0.026)	30
3	9.52(0.1)	6.60(0.040)	50
4	9.52(0.1)	8.55(0.052)	70
5	9.52(0.1)	10.24(0.062)	90
6[a]	9.52(0.1)	10.24(0.062)	90

[a] TiO_2 was added to Ti crucible

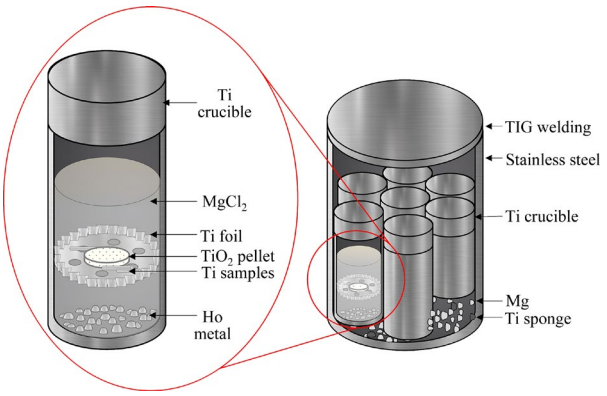

Fig. 6 Schematic diagram of experimental apparatus [31]

In the experiment, Ho was first placed at the bottom of a Ti crucible, and a small amount of $MgCl_2$ molten salt was added to cover the metal. $HoCl_3$ and the Mg-reducing agent were produced by the chemical reaction shown in Eq. (18) to prepare the $MgCl_2$−$HoCl_3$ molten salt. At the same time, the Ti foil was placed above the Ho metal, and Ti and TiO_2 were arranged on the Ti foil as required. The remaining molten salt was then placed in a Ti crucible. Each Ti crucible was then placed in a stainless-steel crucible. Approximately 20 g of the Ti sponge was added to the stainless-steel crucible to absorb water and residual O, and 5 g of Mg was added to ensure sufficient reducing agent. Finally, the stainless-steel crucible was welded and sealed using Ar arc welding, placed in a muffle furnace, heated to the target temperature, and maintained at that temperature for 48 h. After 48 h, the stainless-steel crucible was removed and quenched in water, and the cover was cut to remove the Ti sample from the crucible.

$$Ho(s)+3/2MgCl_2(l)=HoCl_3(l)+3/2Mg(l) \quad (18)$$

After the experiment, the Ti samples were chemically etched with HF−HNO_3−H_2O (1:4:10 in volume ratio) to remove residual salts and deoxidization products (HoOCl) from their surfaces, and then washed with distilled water, alcohol, and acetone. After drying, the O concentration in each Ti sample was determined using an oxygen and nitrogen analyzer (LECO TC−400). In addition, the reduced Ti sheet was immersed in deionized water and HCl solution to remove the molten salt, Mg, MgO, and HoOCl from its surface, and its phase composition was determined by X-ray diffractometry (XRD; Rigaku). The microstructures and elemental concentrations were characterized by scanning electron microscopy (SEM; Hitachi).

4 Results and discussion

4.1 Thermochemical deoxidation

Table 4 presents the experimental conditions for the thermochemical deoxidation and the O concentrations of the Ti samples before and after the experiment. The holding time was determined using the diffusion coefficient of β-Ti. The holding time of the thermochemical deoxidation experiment was 48 h, which was sufficient to allow the deoxidation reaction to reach Mg−$MgCl_2$−$HoCl_3$−HoOCl equilibrium. The essentially identical O concentrations of the Ti samples with different initial O concentrations (Ti-A 9.60×10^{-4}; Ti-B 1.30×10^{-3}) after the experiments confirm that he deoxidation reaction reached equilibrium. The activity of $HoCl_3$ (a_{HoCl_3}) is defined as $a_{HoCl_3}=n_{HoCl_3}/(n_{HoCl_3}+n_{MgCl_2})$, where n_{HoCl_3} and n_{MgCl_2} are amounts (in mol) of $HoCl_3$ and $MgCl_2$, respectively.

As shown in Table 4, the O concentration in the Ti samples (Ti-A and Ti-B) decreased after the thermochemical deoxidation. This indicates the feasibility of removing the solid dissolved O from Ti using Mg in the $MgCl_2$−$HoCl_3$ molten salt. However, at $HoCl_3$ activity of 0.1, the O concentration in the Ti sample is marginally higher than the initial concentration because of the low activity of $HoCl_3$ and the residual O in the crucible reacting with the Ti sample. Additionally, between 1023 and 1073 K, the O concentrations of the Ti samples with different initial O concentrations (Ti-A 9.60×10^{-4}; Ti-B 1.30×10^{-3}) at a given temperature and the $HoCl_3$ activity remain essentially unchanged after the deoxidation

treatment. This indicates that the Mg−$MgCl_2$−HoOCl−$HoCl_3$ equilibrium was reached in the system. These results demonstrate that 48 h is sufficient for the deoxidation reaction to reach equilibrium. Using the results shown in Table 4, the variation in the O concentration of the Ti samples with $HoCl_3$ activity was plotted, as shown in Fig. 7.

As shown in Table 4 and Fig. 7, at a given temperature, the O concentration of the Ti samples decreases continuously as the activity of $HoCl_3$ increases from 0.1 to 0.9 (Experiments $1^{\#}$–$5^{\#}$). This indicates that the higher activity of $HoCl_3$ in the system results in a lower deoxidation limit from 1073 to 1223 K. Using 1173 K as an example, when the activities of $HoCl_3$ are 0.1, 0.3, 0.5, 0.7, and 0.9, the O concentrations in the Ti-A samples are 8.30×10^{-4}, 7.70×10^{-4}, 7.60×10^{-4}, 7.30×10^{-4}, and 3.30×10^{-4}, respectively, and those in the Ti-B samples are 1.40×10^{-3}, 1.30×10^{-3}, 1.10×10^{-3}, 9.00×10^{-4}, and 4.10×10^{-4}, respectively. Together with the thermodynamic analysis, these results demonstrate that $HoCl_3$ effectively reduces the activity of MgO in the system. The higher the $HoCl_3$ activity, the lower the O concentration in the Ti samples and the better the deoxidation effect.

4.2 Reduction of TiO_2

The feasibility of using $HoCl_3$ in a $MgCl_2$−$HoCl_3$ molten salt to assist Mg deoxidation was demonstrated. To investigate the feasibility of using the $HoCl_3$-assisted magnesiothermic reduction of TiO_2 to prepare low-O Ti powder, a thermal reduction experiment ($HoCl_3$ activity of 0.9) was conducted.

Table 4 Experimental results of thermochemical equilibrium deoxidation

Activity of $HoCl_3$	Type of Ti samples	O concentration/10^{-6}						
		Initial	1023 K	1073 K	1123 K	1173 K	1223 K	1273 K
0.1	Ti-A	960	980	2500	980	830	2800	2000
	Ti-B	1300	1100	1200	1100	1400	4000	2900
0.3	Ti-A	960	950	1200	950	770	3500	980
	Ti-B	1300	1000	1200	1000	1300	1720	1000
0.5	Ti-A	960	750	1000	750	760	980	780
	Ti-B	1300	1000	1700	980	1100	700	690
0.7	Ti-A	960	660	600	660	730	800	650
	Ti-B	1300	620	1000	620	900	674	700
0.9	Ti-A	960	660	770	620	330	403	710
	Ti-B	1300	410	890	720	410	577	570

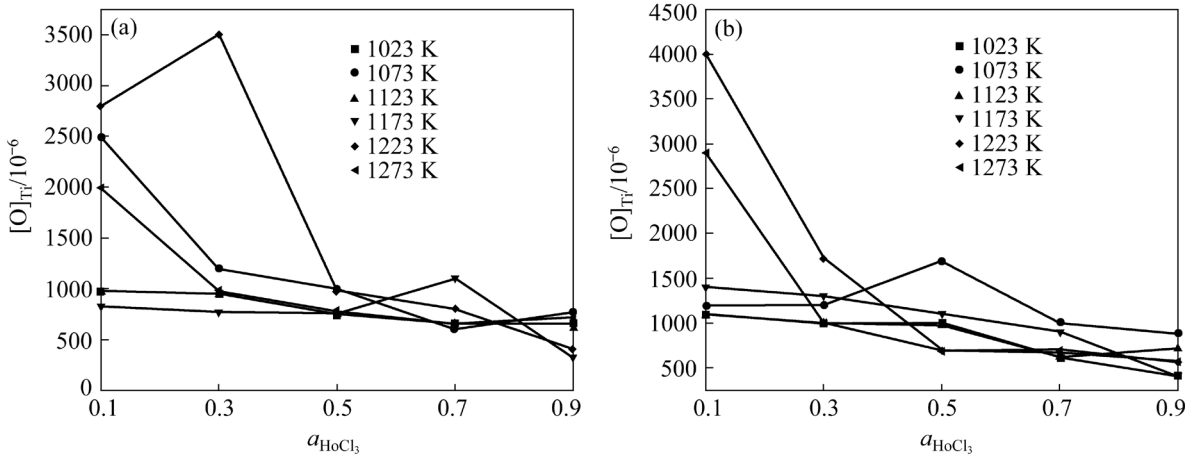

Fig. 7 Relationship between O concentration in Ti ($[O]_{Ti}$) and activity of $HoCl_3$ (a_{HoCl_3}): (a) Ti-A; (b) Ti-B

Figure 8 [31] shows the XRD patterns of TiO_2 before and after sintering. As shown in Fig. 8, the phase of the material before and after sintering corresponds to TiO_2.

Figure 9 shows the XRD patterns of the products from Experiment 6# after pickling for the a_{HoCl_3} of 0.9 at 1023, 1073, 1123, 1173, 1223, and 1273 K.

The presence of Ti in the experimental product, as shown in Fig. 9, demonstrates the feasibility of preparing Ti powder through the magnesiothermic reduction of TiO_2. However, a byproduct, HoOCl, is also detected, for which no suitable removal method has yet been developed. Figure 9 also shows that during the reaction, the $HoCl_3$ molten salt effectively reduces the activity of MgO in the system ($MgO(s)+HoCl_3(l)=HoOCl(s)+MgCl_2(l)$)

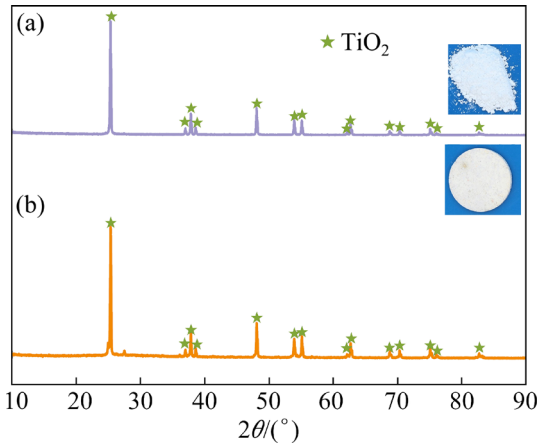

Fig. 8 XRD patterns of TiO_2 before (a) and after (b) sintering [31]

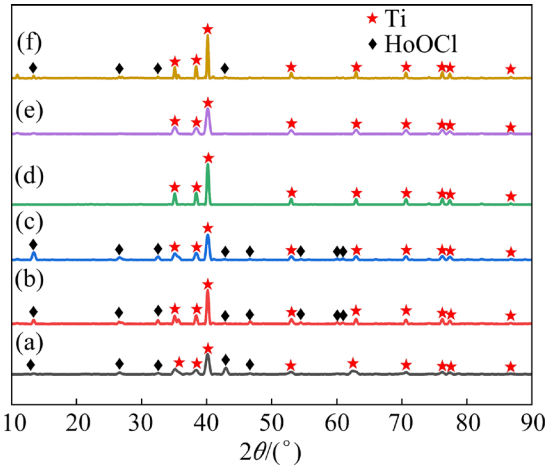

Fig. 9 XRD patterns of products prepared at 1023 K (a), 1073 K (b), 1123 K (c), 1173 K (d), 1223 K (e), and 1273 K (f)

and HoOCl is generated. This allowed the $Mg–MgCl_2–HoCl_3–HoOCl$ equilibrium to be achieved and promoted reduction and deoxidation. In this study, the O concentration in the Ti powder was determined by measuring the O concentration in the Ti sample. Table 5 presents the experimental reduction conditions and the O concentrations in the Ti samples before and after the experiment.

Table 5 O concentrations of Ti samples after reduction experiment

Experimental condition	Activity of $HoCl_3$	Type of Ti samples	O concentration/10^{-6}	
			Initial	After experiment
1023 K, 48 h	0.9	Ti-A	960	480
1073 K, 48 h	0.9	Ti-A	960	390
1123 K, 48 h	0.9	Ti-A	960	350
1173 K, 48 h	0.9	Ti-A	960	200
1223 K, 48 h	0.9	Ti-A	960	210
1273 K, 48 h	0.9	Ti-A	960	220

As shown in Table 5, when the activity of $HoCl_3$ was 0.9 in Experiment 6#, the O concentrations of the Ti samples are lower than 4.00×10^{-4} between 1073 and 1223 K. This indicates that the preparation of low-O Ti powder by the magnesiothermic reduction of TiO_2 is feasible.

Figure 10 shows SEM images of experimental products when the activity of $HoCl_3$ is 0.9 at 1073−1223 K. Table 6 presents the results of the EDS point-scan analysis.

As shown in Fig. 10 and Table 6, the proportion of Ti in the products is considerably high, particularly within the temperature range of 1173−1223 K. The Ti content is 100%. This proves that in the $MgCl_2–HoCl_3$ molten salt system, Mg can reduce TiO_2 to low-O Ti powder. The presence of small amounts of Ho, Cl, and O at some points is due to the experimental by-product of HoOCl. The presence of HoOCl further demonstrats that the $HoCl_3$ molten salt effectively reduced the activity of MgO and promoted the reaction between Mg and O in Ti. This mechanism is illustrated in Fig. 11 [32].

During the magnesiothermic reduction process, the MgO by-product adhered to the reactant surface, thereby hindering the reaction. Although Ti powder could be prepared, its O concentration was typically

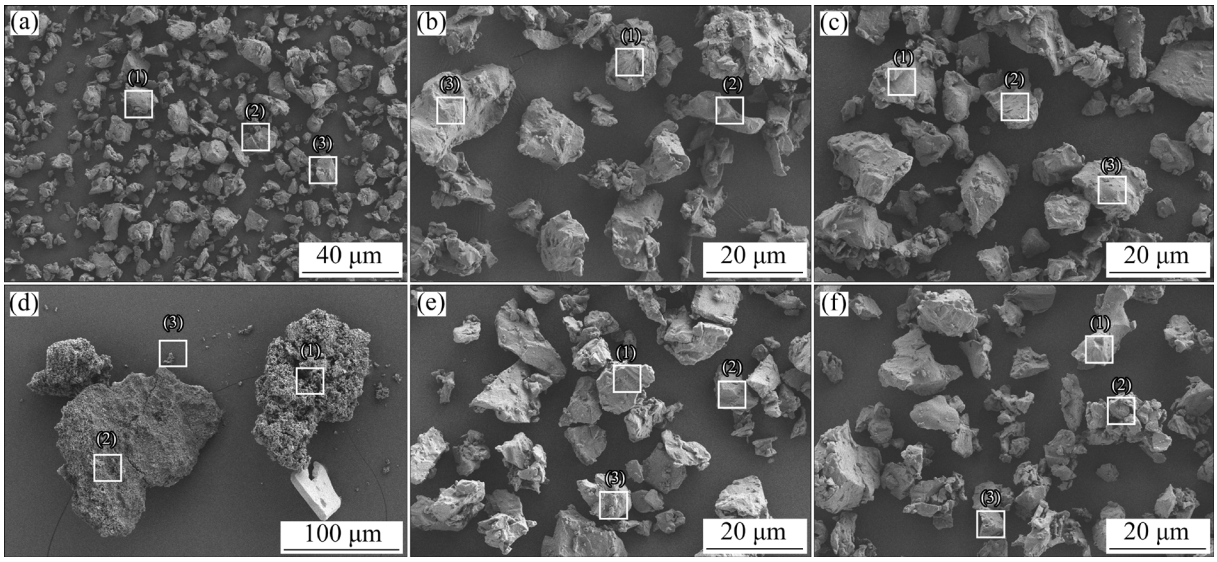

Fig. 10 SEM images of experimental products obtained at different temperatures: (a) 1023 K; (b) 1073 K; (c) 1123 K; (d) 1173 K; (e) 1223 K; (f) 1273 K

Table 6 Types and element contents in TiO_2 reduction products

Experimental condition	Point No. in Fig. 10	Element content/wt.%			
		Ti	O	Ho	Cl
1023 K, 48 h	(1)	97.0	1.3	0.2	1.5
	(2)	99.0	0.2	0.8	0
	(3)	97.0	2.0	1.0	0
1073 K, 48 h	(1)	98.0	1.8	0.2	0
	(2)	99.0	0.2	0.8	0
	(3)	97.0	2.0	1.0	0
1123 K, 48 h	(1)	99.8	0	0.2	0
	(2)	99.4	0	0.3	0.3
	(3)	98.2	0.8	0.6	0.4
1173 K, 48 h	(1)	99.9	0	0.1	0
	(2)	100.0	0	0	0
	(3)	99.8	0	0.2	0
1223 K, 48 h	(1)	99.8	0	0	0.2
	(2)	99.9	0	0.1	0
	(3)	100.0	0	0	0
1273 K, 48 h	(1)	100.0	0	0	0
	(2)	99.0	0.6	0.1	0.3
	(3)	99.6	0	0.2	0.2

higher than 1.00×10^{-2}. As shown in Fig. 11, the activity of MgO can be effectively reduced with the aid of a $HoCl_3$ molten salt ($MgO(s)+HoCl_3(l)=HoOCl(s)+MgCl_2(l)$). Thus, TiO_2 reduction and deoxidization can be combined to prepare low-O Ti powder via the one-step reduction of TiO_2.

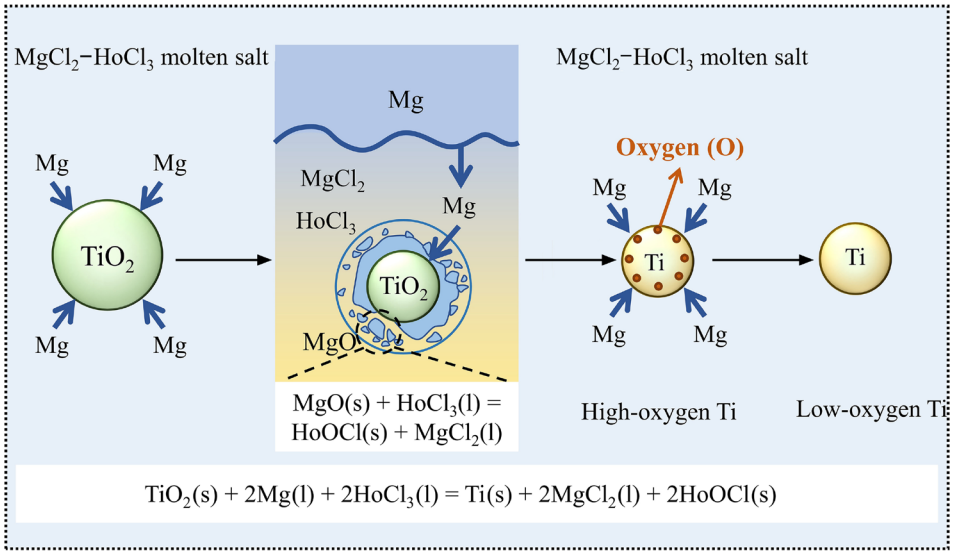

Fig. 11 Mechanism of magnesiothermic reduction of TiO_2 assisted by $HoCl_3$ molten salt [32]

5 Conclusions

(1) Thermodynamic calculations demonstrated the feasibility of preparing Ti powder through the magnesiothermic reduction of TiO_2 between 1023 and 1273 K. The presence of MgO during the reduction process hindered reduction reactions. The MgO activity was effectively reduced by adding $HoCl_3$ to the system. Consequently, low-O Ti powder can be prepared when Mg−$MgCl_2$−HoOCl−$HoCl_3$ equilibrium is reached.

(2) Low-O Ti powders with O concentrations of less than 5.00×10^{-4} were experimentally obtained within the temperature range of 1023−1273 K.

(3) Based on the aforementioned theoretical and experimental results, a new process for preparing low-O Ti powder by the one-step reduction of TiO_2 was proposed. This method provides support for technological progress and innovation in the Ti industry.

CRediT authorship contribution statement

Li-guo ZHU: Investigation, Methodology, Writing − Origin-draft, Writing − Review & editing; **Chong-lin BAI:** Investigation; **Ling-xin KONG:** Conceptualization, Funding acquisition, Supervision, Writing – Review & editing; **Bin YANG:** Supervision, Writing – Review & editing; **Bao-qiang XU:** Validation.

Declaration of competing interest

The authors declare that they have no known competing financial interests or personal relationships that could have appeared to influence the work reported in this paper.

Acknowledgments

This study was financially supported by the National Natural Science Foundation of China (No. 21968013). The authors are grateful to Professors Toru H. OKABE and Takanari OUCHI at The University of Tokyo for their invaluable suggestions and technical assistance.

References

[1] U.S. Geological Survey. Mineral commodity summaries 2023 [R]. Washington DC: Department of the Interior, U.S. Geological Survey, 2023.

[2] ZHANG Yi-neng, YANG Hai-lin, JUAIM A N, CHEN Xiao-na, LU Chang, ZOU Ling, WANG Yin-zhou, ZHOU Xiong-wen. Biocompatibility and osteogenic activity of Zr−30Ta and Zr−25Ta−5Ti sintered alloys for dental and orthopedic implants [J]. Transactions of Nonferrous Metals Society of China, 2023, 33(3): 851−864.

[3] YU Ai-hua, XU Wei, LU Xin, TAMADDON M, LIU Bo-wen, TIAN Shi-wei, ZHANG Ce, MUGHAL M A, ZHANG Jia-zhen, LIU Chao-zong. Development and characterizations of graded porous titanium scaffolds via selective laser melting for orthopedics applications [J]. Transactions of Nonferrous Metals Society of China, 2023, 33(6): 1755−1767.

[4] ZHANG Fang-zhou, WANG Bo, CAO Qing-hua, ZHANG Li, ZHANG Hao-yang. Effect of deformation degree on microstructure and mechanical properties evolution of TiB_w/Ti60 composites during isothermal forging [J].

Transactions of Nonferrous Metals Society of China, 2023, 33(3): 802−815.

[5] KROLL W. The production of ductile titanium [J]. Transactions of the Electrochemical Society, 1940, 78: 35.

[6] GANDEVIA S C, PHEGAN C M L. Perceptual distortions of the human body image produced by local anaesthesia, pain and cutaneous stimulation [J]. Journal of Physiology, 1999, 514: 609−616.

[7] TANAKA T, OUCHI T, OKABE T H. Lanthanothermic reduction of TiO_2 [J]. Metallurgical and Materials Transactions B, 2020, 51: 1485−1494.

[8] SEETHARAMAN S, MCLEAN A, GUTHRIE R, SRIDHAR S. Thermodynamic aspects of process metallurgy [M]. Amsterdam: Elsevier, 2014.

[9] XIA Yang, ZHAO Jin-long, TIAN Qing-hua, GUO Xue-yi. Review of the effect of oxygen on titanium and deoxygenation technologies for recycling of titanium metal [J]. JOM, 2019, 71: 3209−3220.

[10] ZHANG Ying, FANG Z Z, SUN Pei, ZHENG Shi-li, XIA Yang, FREE M. A perspective on thermochemical and electrochemical processes for titanium metal production [J]. JOM, 2017, 69: 1861−1868.

[11] FANG Z Z, PARAMORE J D, SUN Pei, CHANDRAN K S R, ZHANG Ying, XIA Yang, CAO Fei, KOOPMAN M, FREE M. Powder metallurgy of titanium—Past, present, and future [J]. International Materials Reviews, 2018, 63: 407−459.

[12] LI Qing, ZHU Xiao-fang, ZHANG Ying, FANG Z Z, ZHENG Shi-li, SUN pei, XIA Yang, LI Ping, ZHANG Yang, ZOU Xing. An investigation of the reduction of TiO_2 by Mg in H_2 atmosphere [J]. Chemical Engineering Science, 2019, 195: 484−493.

[13] LEFLER H, FANG Z Z, ZHANG Ying, SUN Pei, XIA Yang. Mechanisms of hydrogen-assisted magnesiothermic reduction of TiO_2 [J]. Metallurgical and Materials Transactions B, 2018, 49(6): 2998−3006.

[14] ZHAO Kun, FENG Nai-xiang. Rare metal technology [M]. Berlin: Springer, 2017: 167−175.

[15] HARTMAN A D, GERDEMANN S J, HANSEN J S. Producing lower-cost titanium for automotive applications [J]. JOM, 1998, 50: 16−19.

[16] ZHANG Ying, FANG Z Z, XIA Yang, SUN Pei, DEVENER B V, FREE M, LEFLER H, ZHENG Shi-li. Hydrogen assisted magnesiothermic reduction of TiO_2 [J]. Chemical Engineering Journal, 2017, 308: 299−310.

[17] SUZUKI R O, INOUE S. Calciothermic reduction of titanium oxide in molten $CaCl_2$ [J]. Metallurgical and Materials Transactions, 2003, 34: 287−295.

[18] OKABE T H, ODA T, MITSUDA Y. Titanium powder production by preform reduction process (PRP) [J]. Journal of Alloys and Compounds, 2004, 364: 156−163.

[19] JIA Jin-gang, XU Bao-qiang, YANG Bin, WANG Dong-sheng, LIU Da-chun. Preparation of titanium powders from TiO_2 by calcium vapor reduction [J]. JOM, 2013, 65: 630−635.

[20] XU Bao-qiang, YANG Bin, JIA Jin-gang, LIU Da-chun, XIONG Heng, DENG Yong. Behavior of calcium chloride in reduction process of titanium dioxide by calcium vapor [J]. Journal of Alloys and Compounds, 2013, 576: 208−214.

[21] WAN He-li, XU Bao-qiang, DAI Yong-nian, YANG Bin, LIU Da-chun, SEN Wei. Preparation of titanium powders by calciothermic reduction of titanium dioxide [J]. Journal of Central South University, 2012, 19: 2434−2439.

[22] ZHOU Xin-yu, DOU Zhi-he, ZHANG Tin-an, YAN Ji-sen, YAN Jian-peng. Preparation of low-oxygen Ti powder from TiO_2 through combining self-propagating high temperature synthesis and electrodeoxidation [J]. Transactions of Nonferrous Metals Society of China, 2022, 32: 3469−3477.

[23] NERSISYAN H H, WON H I, WON C W, JO A, KIM J H. Direct magnesiothermic reduction of titanium dioxide to titanium powder through combustion synthesis [J]. Chemical Engineering Journal, 2014, 235: 67−74.

[24] FAN Shi-gang, DOU Zhi-he, ZHANG Ting-an, YAN Ji-sen. Self-propagating reaction mechanism of Mg–TiO_2 system in preparation process of titanium powder by multi-stage reduction [J]. Rare Metals, 2021, 40: 2645−2656.

[25] WENZ D A, JOHNSON I, WOLSON R D. $CaCl_2$-rich region of the $CaCl_2$−CaF_2−CaO system [J]. Journal of Chemical and Engineering Data, 1969, 14: 250−252.

[26] EMSLEY J. Nature's building blocks: An AZ guide to the elements [M]. New York: Oxford University Press, 2011.

[27] GUPTA C K, KRISHNAMURTHY N. Extractive metallurgy of rare earths [J]. International Materials Reviews, 1992, 37: 197−248.

[28] KONG L X, OUCHI T, OKABE T H. Direct deoxidation of Ti by Mg in $MgCl_2$−$HoCl_3$ flux [J]. Materials Transactions, 2019, 60: 2059−2068.

[29] BARIN I. Thermochemical data of pure substances [M]. 3nd ed. Weinheim: VCh, 2008.

[30] OKABE T H, SUZUKI R O, OISHI T, KATSUTOSHI O. Thermodynamic properties of dilute titanium-oxygen solid solution in beta phase [J]. Materials Transactions, JIM, 1991, 32: 485−488.

[31] ZHU Li-guo, KONG Ling-xin, Bai Chong-lin, XU Bao-qiang, YANG Bin. Preparation of low-oxygen titanium powder by magnesiothermic reduction of TiO_2 in KCl−$MgCl_2$−YCl_3 molten salt [J]. Journal of Materials Research and Technology, 2023, 25: 4929−4941.

[32] ZHU Li-guo, ZAHNG Zu-qing, KONG Ling-xin, WANG Cheng-yuan, YANG Bin, XU Bao-qiang. Production of low-oxygen Ti powder by magnesiothermic reduction of TiO_2 in $MgCl_2$−KCl−$CeCl_3$ molten salt [J]. Metallurgical and Materials Transactions B, 2024. https://doi.org/10.1007/s11663-024-03251-7.

$MgCl_3$−$HoCl_3$ 熔盐辅助镁热还原 TiO_2 制备低氧钛粉

朱立国[1,2,3,4]，白崇霖[1,2,3,4]，孔令鑫[1,2,3,4]，杨 斌[1,2,3,4]，徐宝强[1,2,3,4]

1. 昆明理工大学 云南省有色金属真空冶金重点实验室，昆明 650093；
2. 昆明理工大学 省部共建复杂有色金属资源清洁利用国家重点实验室，昆明 650093；
3. 昆明理工大学 真空冶金国家工程研究中心，昆明 650093；
4. 昆明理工大学 冶金与能源工程学院，昆明 650093

摘 要：为了降低钛的生产成本，提出一种 $MgCl_2$−$HoCl_3$ 熔盐辅助镁热还原 TiO_2 直接制备低氧钛粉的新方法。热力学计算表明，镁热还原 TiO_2 是可行的。然而，还原副产物氧化镁阻碍了还原反应的进行，导致钛粉的氧含量较高。往体系中加入 $HoCl_3$ 显著降低了 MgO 的活性，从而制备低氧钛粉。在 1023~1273 K 下，以 $MgCl_2$−$HOCl_3$ 为熔盐，开展热化学脱氧和还原实验研究。结果表明，在 Mg−$MgCl_2$−HoOCl−$HoCl_3$ 平衡条件下可以制备氧含量低于 5.00×10^{-4} (质量分数) 的钛粉。

关键词：钛粉；$MgCl_2$−$HoCl_3$ 熔盐；TiO_2；HoOCl；镁热还原

(Edited by Wei-ping CHEN)